Computational and Structural Biotechnology Journal 18 (2020) 3447–3456

COMPUTATIONAL AND STRUCTURAL BIOTECHNOLOGY JOURNAL

journal homepage: www.elsevier.com/locate/csbj

Dominance network analysis of the healthy human vaginal microbiome not dominated by *Lactobacillus* species

Wendy Li [a,c], Zhanshan (Sam) Ma [a,b,c,*]

[a] *Computational Biology and Medical Ecology Lab, State Key Laboratory of Genetic Resources and Evolution, Kunming Institute of Zoology, Chinese Academy of Sciences, Kunming, China*
[b] *Center for Excellence in Animal Evolution and Genetics, Chinese Academy of Sciences, Kunming 650223, China*
[c] *Kunming College of Life Sciences, University of Chinese Academy of Sciences, China*

ARTICLE INFO

Article history:
Received 3 June 2020
Received in revised form 29 October 2020
Accepted 30 October 2020
Available online 10 November 2020

Keywords:
Non-*Lactobacillus* dominated vaginal microbiome (nLDVM)
Dominance network (DN)
Gardnerella
Lactobacillus iners
Core-periphery network
High salience skeleton network

ABSTRACT

Although *Lactobacillus* dominance is one of the commonest characteristics of many healthy vaginal microbiomes, a significant proportion of healthy women lack an appreciable amount of *Lactobacillus* in their microbiome. Indeed, the vaginal microbiomes of many BV (bacterial vaginosis) patients lack the dominance by *Lactobacillus*. One would wonder what are special with those healthy non-Lactobacillus dominated vaginal microbiomes (nLDVM)? Here we re-analyzed the vaginal microbiome datasets of 1107 postpartum women in rural Malawi Doyle et al. (2018) using species dominance network (SDN) analysis. We discovered that: (*i*) The DN of the nLDVM is predominantly mutualistic, where most competitive (negative) relationships were from bacterial vaginosis-associated bacteria (BVAB), >60% occurred between BVAB and non-BVAB genera. *Gardnerella* was inhibited by a mutualistic combination of 23 genera, and *Lactobacillus* by 15 genera. These may be possible mechanisms by which the microbiome maintains high diversity but avoids dominance by *Gardnerella* or *Lactobacillus*. *Gardnerella* and *Lactobacillus* were only cooperated with a few genera, but they were positively connected with each other. The suppressed *Lactobacillus* species positively associated with *Gardnerella* was *Lactobacillus iners*, indicating that *L. iners* might act as an "enemy" in the *Lactobacillus*-poor vaginal microbiome, and inhibition of *Gardnerella* and *L. iners* might be a self-protective mechanism to maintain stability and health of this microbiome. (*ii*) We identified skeletons of the DNs and separate pathways consisting of high salience skeletons. *Finegoldia* species and *Staphylococcus epidermidis* were the hubs of the skeleton network. The roles that they play in the nLDVM deserve more attention of future studies.

1. Introduction

Indigenous vaginal microbiomes can strongly influence host health. *Lactobacillus* species are the dominant vaginal bacterial species in most reproductive-aged women and play a key role in maintaining the stability of the vaginal environment, e.g., producing lactic acid to maintain low pH (3.5–4.5). Thus, *Lactobacillus*-dominated microbiomes have long been considered a sign of vaginal health. However, this assumption has been challenged in recent years with the development of sequencing technology and culture-independent analysis. Ravel et al. [39] divided the human vaginal microbiome into five major community state types (CSTs) based on analysis of healthy American women from four ethnic groups (i.e., white, black, Hispanic, and Asian), with CSTs I, II, III, and V dominated by *Lactobacillus* spp., and CST IV, which is more common in black and Hispanic women, composed of facultative or strictly anaerobic bacteria, such as *Gardnerella*, *Atopobium*, *Mobiluncus*, *Prevotella*, *Streptococcus*, and *Sneathia* [39,13]. Based on analysis of African American and European women, Fettweis et al. [11] also noted that ethnicity can influence the composition of the vaginal microbiome. Furthermore, Anahtar et al. [1] noted that non-*Lactobacillus* dominated vaginal microbiomes (nLDVM) are found in 63% of healthy South African women, with 45% dominated by *Gardnerella*.

In addition to ethnicity, the definition of a normal vaginal microbiome has also been challenged by other factors, such as pregnancy. Recent studies have found that the vaginal microbiome

* Corresponding author at: Computational Biology and Medical Ecology Lab, State Key Laboratory of Genetic Resources and Evolution, Kunming Institute of Zoology, Chinese Academy of Sciences, Kunming, China.
E-mail address: ma@vandals.uidaho.edu (Zhanshan (Sam) Ma).

https://doi.org/10.1016/j.csbj.2020.10.033

is more stable during pregnancy and decreases in diversity with an increase in *Lactobacillus* spp. [41,8]. In addition, radical changes in the *Lactobacillus*-deficient vaginal community have been observed in postpartum women, which can persist up to a year after delivery [8]. Recently, Doyle et al. [9] sampled and characterized the vaginal microbiomes of 1107 rural postpartum Malawi women, and found that 76% microbiome communities were non-*Lactobacillus* dominated with a dominance of *Gardnerella* spp., i.e., *Gardnerella vaginalis.* Furthermore, although *Lactobacillus* species increased with time from delivery, *Gardnerella* spp. remained a major part in the vaginal microbiome of these postpartum women [9].

Both the structure and composition of the vaginal microbiome are associated with disease risk, e.g., bacterial vaginosis (BV) and AIDS, as well as preterm birth [2,6,14,19,20,23,41,45]. As the most common vaginal dysbiosis, BV is characterized by changes in a *Lactobacillus*-dominated microbiome to a mixed multispecies community, with the increase in species diversity and anaerobic microorganisms [40,35]. Possible agents of BV include *Gardnerella*, *Atopobium*, *Prevotella*, *Peptostreptococcus*, *Mobiluncus*, *Sneathia*, *Leptotrichia*, *Mycoplasma*, and BV-associated bacteria (BVAB1, BVAB2, and BVAB3) [12,35]. Due to the development of molecular methods in recent years, the list of BV-associated bacteria (BVAB) continues to expand. Gosmann et al. [14] identified that healthy South African women with highly diverse and anaerobic-dominated vaginal microbiomes had a higher risk of HIV than women with *Lactobacillus*-dominated microbiomes. They also found that *Prevotella*, *Sneathia*, and other anaerobes were associated with an increase in HIV infection. In addition, studies on the vaginal microbiome during pregnancy have demonstrated an association between preterm birth and microbiomes with a high abundance of *Gardnerella* [8,6].

To date, however, studies on the vaginal microbiome have not clearly defined normal or optimal microbial communities, nor provided a rigorous concept of BV. BV is caused by dysbiosis of the vaginal microbiome, which more often manifests as dysfunction rather than just a change in species composition. In the present study, we re-analyzed a large dataset of vaginal microbiome samples collected from 1107 postpartum women in rural Malawi, with most of these microbiomes reported to be non-*Lactobacillus* dominated [9]. Our analysis aimed to investigate what are special with those healthy nLDVMs in terms of the critical network structures responsible for preventing dysbiosis associated with BV. In other words, how do these non-*Lactobacillus*, healthy vaginal microbiomes maintain their stability or resilience? We utilized the framework for exploring diversity-stability relationships proposed by Ma & Ellison [26] to implement the reanalysis of the Doyle et al. [9] dataset, including (*i*) basic DN analysis; (*ii*) core/periphery network (CPN) analysis; and (*iii*) high salience skeleton network (HSN) analysis.

2. Materials and methods

2.1. Vaginal microbiome dataset

The 16S rRNA dataset was based on vaginal microbiome samples collected from 1107 rural Malawi women after delivery [9]. Most samples were collected within the first 20 d of delivery but ranged from 5 to 583 d post-delivery. The samples were sequenced with 16S-rRNA amplicon sequencing technology. Sequencing data were processed using dada2 plugin in qiime2 v2019-08, including quality trimming, denoising, merging, and chimera detection. These processes were done using dada2 plugin with default setting. After quality control, the sequences were clustered into operational taxonomic units (OTUs) using qiime feature-classifier classify-sklearn plugin. In this study, a total of 1076 samples with more than 2000 reads were retained for network analysis. More detailed information on the dataset is provided in Doyle et al. [9].

2.2. Dominance network (DN) analysis

The computational procedures for DN construction and analysis of the vaginal microbiome of the postpartum women followed [25,26]. To reduce the noise effect of OTUs with extremely low abundance or potentially spurious OTU reads, we filtered those OTUs whose total reads in all 1076 samples were less than 1000, i.e., approximately one read per sample. This was equivalent to removing so-called singletons, which is a common practice in ecological analysis. After filtering, 360 OTUs annotated to genus and species were retained for the following analyses. In addition, we combined the OTUs that belonged to the same genus into a new OTU and obtained 60 new OTUs at the genus level. We constructed two DNs based on 60 genus OTUs and the top 120 species OTUs by dominance value, respectively. The dominance values of OTUs were utilized to construct a species correlation network based on Spearman's rank correlation coefficients (R) [25,26,27,28,21]. Correlation relationships with a p-value of $\leq$0.001 after false discovery rate (FDR) adjustment were set as the criteria for selecting network edges (links). Cytoscape software (Version 2.8.3) was used to visualize the networks and the iGraph R-package was utilized for computing network properties [4,44]. We also detected the positive-to-negative links (P/N) ratio[24]in the DNs.

2.3. Core/periphery network (CPN) analysis

According to Csermely et al. [7], a perfect or ideal CPN consists of a fully linked core and a periphery that is fully connected to the core, but with no peripheral nodes connected to each other. Formally, let $G = (V, E)$ be an undirected, unweighted graph with n nodes and m edges, and let $A = (a_{ij})$ be the adjacency matrix of G, where $a_{ij} = 1$ if node i and node j are linked and 0 otherwise. Let δ be a vector of length n with entries of 1 or 0, if the corresponding node belongs to the core or periphery, respectively. Additionally, let $P = (p_{ij})$ be the adjacency matrix of the ideal or perfect CPN of n nodes and m edges. The detection of the core-periphery structure is an optimization problem to find vector δ, such that the objective function (ρ) achieves its maximum based on the following expression:

$$\rho = \sum_{i,j} A_{ij} P_{ij} \tag{1}$$

With vector δ, it is then easy to classify nodes as either core or periphery.

2.4. Microbiome diversity of core and periphery OTUs

Microbiome diversity can be quantified using Hill [16] numbers, as follows:

$${}^{q}D = \left(\sum_{i=1}^{s} p_i^q \right)^{1/(1-q)} \tag{2}$$

where D is diversity, q is the order number of diversity, S is the number of species, and p_i is the dominance value of species i. The diversity order (q) determines the sensitivity of the Hill number to the relative frequencies of species dominance values. When $q = 0$, as species dominance is not involved in the calculation, ${}^{0}D$ is equal to the number of species, or species richness (S). When $q = 1$, species dominance is involved in the calculation and ${}^{1}D$ represents the number of typical or common species in the community, which is equal to the exponential of Shannon entropy. When

q = 2, ^2D is more sensitive to species with high dominance, which is equal to the reciprocal of the Simpson index. Generally, ^qD represents the diversity of a community with $x = {}^qD$ equally dominated species.

2.5. High-salience skeleton network (HSN) analysis

Grady et al. [15] introduced the concept of link salience with consideration of both node degree and link weight, which can be used to classify links into distinct groups. The group containing links with high salience is called a high-salience skeleton and represents the essential links of the network.

Three main steps are followed to determine salience (s_{ij}) of a link between nodes n_i and n_j. First, the shortest path between each pair of nodes in the network is obtained, which represents the path with the shortest total effective distance based on effective proximity d. The effective proximity d of the link (i, j) is $d_{ij} = 1/|\rho_{ij}|$, where ρ_{ij} represents Spearman's correlation coefficient between nodes n_i and n_j. In this step, we can obtain the shortest-path tree (SPT; T(r)) for each node r. If there are N nodes, T(r) is a symmetric $N \times N$, if link (i, j) is part of at least one of the shortest paths, the cell $t_{ij} = 1$, otherwise, $t_{ij} = 0$. We can then linearly superimpose all SPTs, and obtain the salience (S) of the network:

$$S = \langle T \rangle = \frac{1}{N} \sum_r T(r) \tag{3}$$

The S of the network is still a symmetric $N \times N$, in which cell s_{ij} represents the salience of link (i, j). The value of s_{ij} ranges from 0 to 1. The higher the value of s_{ij}, the link (i, j) plays the role in the shortest paths of more nodes.

3. Results

3.1. DN analysis for the nLDVM at the genus level

We used the genus OTUs to build the DN of the nLDVM, which consisted of 60 genera and 531 links. Of the 60 genera, 22 were BVAB, which were identified based on existing literature and were listed in the Table S3 [12,39,13,18,35,42]. The basic network properties are listed in Table S1. The genus *Gardnerella* was either the most abundant OTU (MAO) or the most dominant OTU (MDO) of the genus-level DN. *Corynebacterium* and *Finegoldia* were the hubs in the DN, that are, the OTUs holding the most number of edges. *Gardnerella* and *Corynebacterium* are BVAB OTUs. Fig. 1 displays the genus-level DN of the nLDVM. The BVAB and non-BVAB genera in the DN were divided into two sub-networks in Fig. 1, with the right sub-network consisting of the 21 BVAB genera and the left sub-network consisting of the non-BVAB genera.

The genus-level DN contained 448 positive links and 83 negative links, in which the P/N ratio was 5.398. There were five times more positive correlation relationships than negative correlation relationships, indicating that the nLDVM was predominantly mutualistic. In total, 57.8% (48/83) of negative correlation relationships in this DN were between BVABs and non-BVABs, 34.9% (29/83) were between BVABs, and 7.2% (6/83) were between non-BVABs. This suggested that most competitive (inhibition) relationships in the community were related to BVABs. The average P/N ratio of non-BVAB was 2 times higher than that of BVAB, and the P/N ratios of the non-BVABs were significantly greater than those of the BVABs (Wilcoxon p-value $\leq$0.05). The results demonstrate that the proportion of competition in the relationships held by BVAB genera is significantly higher than that of non-BVAB genera. S3 provides details on the P/N ratios of each genus.

3.2. Core/periphery and nested structures in the genus-level DN

Table S4 lists the main core/periphery/nestedness analysis results for the genus-level DN. The genus-level DN had a strong core-periphery structure (parameter $\rho \approx 0.5$). Half of the nodes were cores (ratio of $c/(c + p)$ = 0.533), i.e., 32 out of 60 genera were cores and 28 were peripheries. Of 32 cores, half were BVAB genera and half were non-BVAB genera. Of 28 peripheries, 6 were BVAB genera and 22 were non-BVAB genera. Table S5 provides details on the core and periphery genera in the DN. In Fig. 1, the nodes in golden and blue represent core and periphery OTUs, respectively. The composition of core OTUs in the DN suggests that BVAB play critical roles in the structural stability of the nLDVM. We also analyzed the diversity of core and periphery genera using Hill numbers (Table S6, Fig. 2). Although the numbers of core and periphery genera were similar in the DN, there were significant differences in their Hill number at diversity order q = 0–3 (Wilcoxon p-value < 0.001) (Table S6). Core diversity was significantly higher than that of the periphery.

The core-core density (B11) was 0.637, which was nearly four times higher than that of the core-periphery (B12(21), density = 0.165) and periphery-periphery (B22, density = 0.177). These results suggest that the interconnections within the core genera were stronger than those between the core and periphery genera or those within the periphery genera. Furthermore, the P/N ratio of the core genera in the DN was five times lower than that of the periphery genera. This can be attributed to the fact that most BVAB were cores that contained many negative links. The nestedness index measures the relative level of nesting degree, where the larger the nestedness index value (ranging from 0 to 1), the higher the nestedness. The S of the DN was 0.437, indicating no strong nesting in this DN.

3.3. High salience skeleton (HSS) network analysis for the nLDVM at the genus level

We performed HSS network analysis to identify the "highways" in the fully connected network of genera. Each link has a salience value ranging from 0 to 1, which can be used to measure the importance of the link. The higher the salience value, the more important the link is to the vaginal microbial community. The HSS results are listed in Table S7. In the fully connected network of genera, 29.6% (524/1770) of links had salience values (S) > 0, 10% (54) had salience values $\geq$ 0.25, and only 3% (16) had salience values $\geq$ 0.5. Fig. 3 shows the network of these skeletons, with a salience value $\geq$ 0.25. The links with salience values $\geq$ 0.5 can be considered as HSSs of the vaginal microbiome. There were 16 HSSs in the network, which were held by 15 non-BVAB OTUs and 8 BVAB OTUs, as listed in Table 1. We further identified seven separate pathways from these 16 HSSs, as shown in Table 2, in which four pathways (#1, #2, #3, and #4) contained three or more nodes and three pathways (#5, #6, and #7) contained two nodes. All HSS-pathways were stringed together by the links with salience values > 0.25.

As the hubs and core of the genus-level DN, *Finegoldia* also had the most skeletons. *Finegoldia* was the members of the #3 HSS-pathway (as shown in Fig. 3 and Table 2). *Staphylococcus* held the most number of HSSs, and these HSSs were part of the #1 pathway. The #1 pathway consisted of 7 genera, in which *Staphylococcus* was the only core and BVAB in the #1 pathway. *Finegoldia* is a genus of Gram-positive bacteria. In the #3 HSS-pathway, *Finegoldia* was positively connected with *Bacteroides* and *Ureaplasma*, which are two BVAB genera. *Bacteroides* is a genus of obligate anaerobic bacteria. *Bacteroides* and *Gardnerella* compose one of the morphotypes to be identified in the Nugent criteria, which has been regarded as the gold standard for BV diagnosis [33,42]. *Ureaplasma* is com-

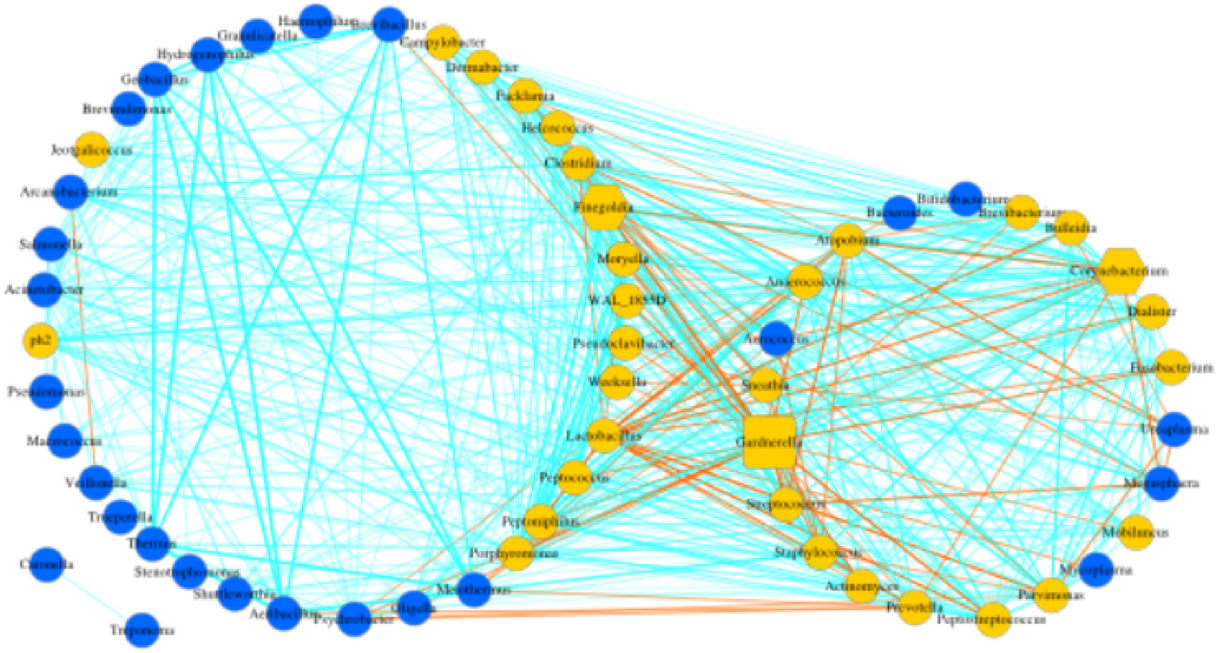

Fig. 1. The DN of non-*Lactobacillus* dominated vaginal microbiome (nLDVM) built based on genera: edges in cyan are positive correlations; edges in orange are negative correlations; the thicker the edge, the stronger the correlated relationship; nodes in gold are core genera; nodes in blue are periphery genera; rectangle represents that the node is both MAO and MDO; and hexagons represent that the nodes are hubs. Hub is the genus that holding the most number of edges. Core represents a set of central, densely connected nodes in the DN, and periphery represents a set of sparsely connected non-central nodes. (For interpretation of the references to colour in this figure legend, the reader is referred to the web version of this article.)

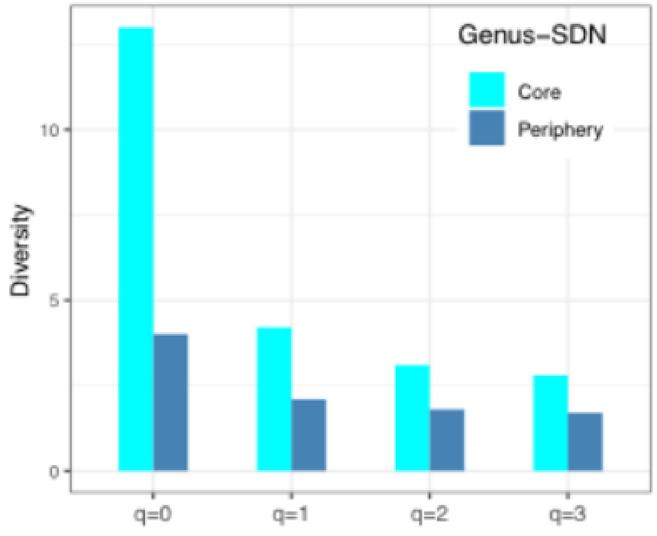

Fig. 2. Diversity in Hill numbers (q = 0–3) of core and periphery OTUs in the genus-level DN: bar in cyan is diversity of core genera; bar in steel blue is diversity of periphery genera. (For interpretation of the references to colour in this figure legend, the reader is referred to the web version of this article.)

monly found in urinary and genital tract, and some *Ureaplasma* spp. such as *U. urealyticum* and *U. parvum* are associated with BV [46,17].

3.4. The DN of the dominant species in the nLDVM

To further explore the relationships between specific species, we subsequently constructed the species-level DN based on the top 120 OTUs by dominance value (accounting for 1/3 of the total species OTUs). The species-level DN is shown in Fig. S1. The MAO, MDO and hub in the species-level DN were *Lactobacillus iners*, *Peptostreptococcus anaerobius* and *Finegoldia*_9698, respectively. The species-level DN was also predominantly mutualistic, in which the P/N ratio was 15.354 (Table S2). 103 out of 113 negative correlations were related to BVAB OTUs, of which 60% (41/103) found between the BVAB and non-BVAB OTUs. The basic network properties are listed in Table S1.

CPN and HSS network analyses were also performed at the species level, and results were listed in Table S4 and Table S7, respectively. The species-level DN had a strong core-periphery structure and a low nested-ness structure, with 45% (53/120) of OTUs belonging to the core. The core-core density was much higher than that of the core-periphery and periphery-periphery density (Fig. S1). These structural attributes were similar to those of the genus-level DN. In the species-level DN, the P/N ratio of the cores was infinite, indicating that there was no negative interaction between core OTUs. We computed the diversity of cores and peripheries in the DN using Hill numbers (Table S6, Fig. S3). When diversity order q = 0 & 1, Hill numbers of cores were significantly less than those of peripheries (Wilcoxon p-value < 0.001), but the difference was not significant between cores and peripheries when q = 2 & 3 (Wilcoxon p-value = 0.540 at q = 2, and = 0.416 at q = 3).

There were 94 skeletons (salience values $\geq$ 0.25) in the species-level DN, of which 22 were considered as the HSSs (salience values $\geq$ 0.5). Fig. S4 displays the network consisting of these skeletons. 8 separate pathways were identified from HSSs, and the details were shown in Table S8. *Finegoldia*_9698 held the most skeletons, and *Staphylococcus epidermidis* held the most HSSs. This finding confirmed our previous analyses on genus level, that *Finegoldia* had the most skeletons and *Staphylococcus* had the most HSSs.

3.5. The roles of Gardnerella and Lactobacillus in the DN

In the genus-level DN, the P/N ratios of the *Gardnerella* and *Lactobacillus* were the lowest, 0.133 and 0.130, respectively, and all other genera were $\geq$ 0.5. The *Gardnerella* held the greatest number

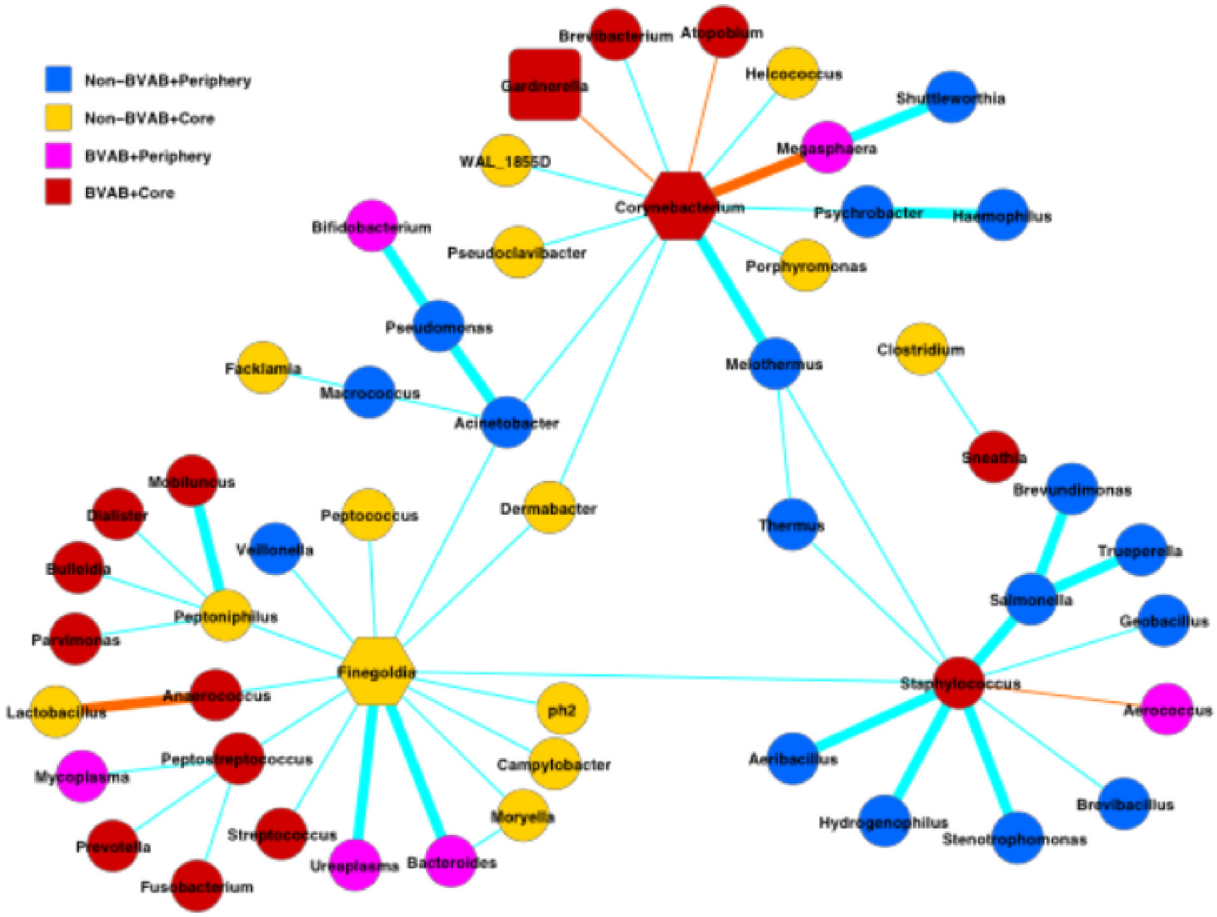

Fig. 3. Skeletons with salience value $S \geq 0.25$ in the genus-level DN: edges in cyan are positive correlation skeletons; edges in orange are negative correlation skeletons; thicker edges are skeletons with salience value $S \geq 0.5$; nodes in blue are non-BVAB periphery genera; nodes in gold are non-BVAB core genera; nodes in magenta are BVAB periphery genera; nodes in deep red are BVAB core genera; hexagons are hubs, and rectangle represents that the node is both MAO and MDO. (For interpretation of the references to colour in this figure legend, the reader is referred to the web version of this article.)

Table 1
High-salience skeletons ($S \geq 0.5$) in the genus-level DN.

ID	Edge with high salience		Salience value (S)	Correlation (R)
1	*Corynebacterium*	*Megasphaera*	0.500	−0.199
2	*Lactobacillus*	*Anaerococcus*	0.517	−0.256
3	*Peptoniphilus*	*Mobiluncus*	0.517	0.294
4	*Staphylococcus*	*Aeribacillus*	0.517	0.315
5	*Finegoldia*	*Bacteroides*	0.550	0.139
6	*Staphylococcus*	*Hydrogenophilus*	0.550	0.292
7	*Corynebacterium*	*Meiothermus*	0.567	0.246
8	*Megasphaera*	*Shuttleworthia*	0.650	0.326
9	*Finegoldia*	*Ureaplasma*	0.683	0.177
10	*Staphylococcus*	*Salmonella*	0.683	0.316
11	*Pseudomonas*	*Acinetobacter*	0.733	0.139
12	*Staphylococcus*	*Stenotrophomonas*	0.783	0.131
13	*Salmonella*	*Brevundimonas*	0.933	0.145
14	*Pseudomonas*	*Bifidobacterium*	0.967	0.115
15	*Psychrobacter*	*Haemophilus*	0.967	0.127
16	*Salmonella*	*Trueperella*	0.967	0.125

of negative links. It was negatively correlated with 23 genera, but was positively correlated with only three, i.e., *Lactobacillus*, *Aerococcus*, and *Atopobium* (Fig. 4A). We termed the sub-network consisting of the 23 genera negatively correlated with *Gardnerella* as the anti-*Gardnerella* cooperative alliance, which all exhibited positive interconnections (Fig. 4B). The structure consisting of *Gardnerella*, *Lactobacillus*, *Aerococcus*, and *Atopobium* was term as the *Gardnerella* cooperative alliance, in which *Atopobium* held positive link with *Aerococcus* and negative link with *Lactobacillus* (Fig. 4C). 11 out of the 26 genera associated with *Gardnerella* were BVAB, including *Aerococcus*, *Atopobium*, *Actinomyces*, *Anaerococcus*, *Corynebacterium*, *Fusobacterium*, *Peptostreptococcus*, *Brevibacterium*, *Staphylococcus*, *Mobiluncus*, and *Streptococcus*, and 7 out of these 11 genera were belonged to the anti-*Gardnerella* cooperative alliance.

Similar to the situation of the *Gardnerella*, the *Lactobacillus* was negatively correlated with 15 genera, but positively correlated only

Table 2
Seven pathways consisting of high-salience skeletons ($S \geq 0.5$) in the genus-level DN.

ID	Pathway	Genera	Num. of genera	Avg. salience value (S)	Core genera	BVAB genera
1	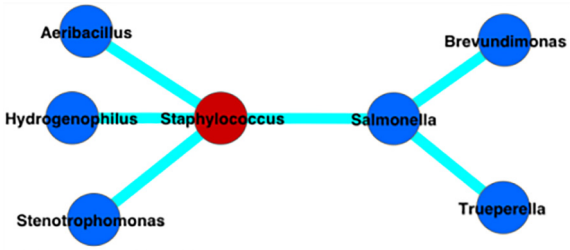	*Brevundimonas Trueperella Salmonella Staphylococcus Aeribacillus Stenotrophomonas Hydrogenophilus*	7	0.739	*Staphylococcus*	*Staphylococcus*
2		*Meiothermus Corynebacterium Megasphaera Shuttleworthia*	4	0.572	*Corynebacterium*	*Corynebacterium Megasphaera*
3		*Bacteroides Finegoldia Ureaplasma*	3	0.617	*Finegoldia*	*Bacteroides Ureaplasma*
4		*Bifidobacterium Pseudomonas Acinetobacter*	3	0.850	–	*Bifidobacterium*
5		*Lactobacillus Anaerococcus*	2	0.517	*Lactobacillus Anaerococcus*	*Anaerococcus*
6		*Peptoniphilus Mobiluncus*	2	0.517	*Peptoniphilus Mobiluncus*	*Mobiluncus*
7		*Psychrobacter Haemophilus*	2	0.967	–	–

Symbols in the second column:

Edges in cyan—positive correlation skeletons
Edges in orange—negative correlation skeletons
Nodes in blue—non-BVAB periphery genera
Nodes in gold—non-BVAB core genera
Nodes in magenta—BVAB periphery genera
Nodes in deep red—BVAB core genera
Hexagons—hubs.

with *Gardnerella* and *Ureaplasma* (Fig. 5A). The 15 genera negatively correlated with *Lactobacillus* formed the anti-*Lactobacillus* cooperative alliance (Fig. 5B), and there were only positively links between them. We term the network consisting of *Lactobacillus, Gardnerella* and *Ureaplasma* as the *Lactobacillus* cooperative alliance (Fig. 5C). 13 genera associated with *Lactobacillus* were BVAB, of which 11 were members of the anti-*Lactobacillus* cooperative alliance.

The DN consisting of the dominant species OTUs contained three OTUs of *Lactobacillu*, i.e., *L. iners*, *Lactobacillus vaginalis* and

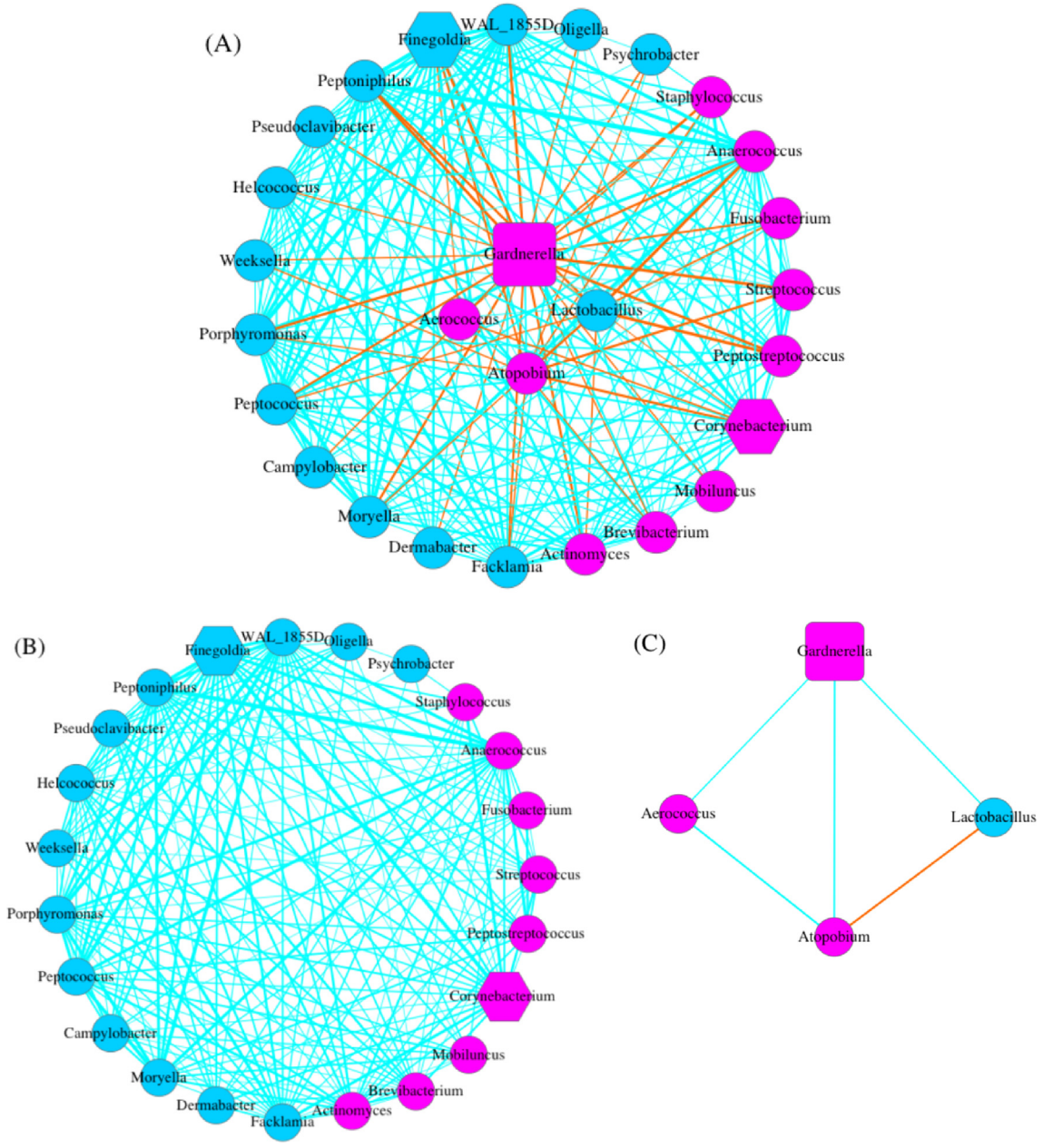

Fig. 4. (A) Sub-network consisting of *Gardnerella* and directly connected genera in the genus-level DN; (B) Anti-*Gardnerella* cooperative alliance: network consisting of genera negatively correlated with *Gardnerella*; (C) *Gardnerella* cooperative alliance: network consisting of genera positively correlated with *Gardnerella*. Edges in cyan are positive correlations; edges in orange are negative correlations; the thicker the edge, the stronger the correlated relationship; nodes in magenta are BVAB genera; nodes in sky blue are non-BVAB genera; rectangle represents that the node is both MAO and MDO; and hexagons represent that the nodes are hubs. (For interpretation of the references to colour in this figure legend, the reader is referred to the web version of this article.)

*Lactobacillus*_12185. They positively interrelated with each other, and held 7 positive and 28 negative links with OTUs of other genera. There were 13 negative links held by *L. vaginalis*, and 15 held by *L. iners*. *L. vaginalis* and *L. iners* negatively associated with 18 OTUs, These OTUs were from 13 genera, including *Actinomyces*, *Anaerococcus*, *Atopobium*, *Bulleidia*, *Clostriduim*, *Dialister*, *Fusobacterium*, *Mycoplasma*, *Parvimonas*, *Peptoniphilus*, *Peptostreptococcus*, *Prevotella* and *Sneathia*, all of which belonged to the anti-*Lactobacillus* cooperative alliance found in the genus-level SCN, and 11 of them were BVAB. Consistent with the anti-*Lactobacillus* cooperative alliance in the genus-level DN, the correlations between these 18 species were all positive. *L. iners* had positive interactions with only three OTUs of other genera, i.e., *Gardnerella*_1521, *Ureaplasma*_13766 and *Veillonella*_8052. *L. vaginalis* was positively correlated with only *Ureaplasma*_13766. These results specifically identified the *Lactobacillus* that was inhibited in the non-*Lactobacillus* dominant vaginal microbiome as *L. vaginalis* and *L. iners*, and their "staunch" allies were *Gardnerella* and *Ureaplasma*. In addition, *Lactobacillus*_12185 held three positive links with *Streptococcus infantis*, *Staphylococcus*_12767 and *Actinetobacter*_7697.

There were 8 OTUs of *Gardnerella* without annotating species name in the species-SCN, and the links between them were all positive. *Gardnerella* OTUs held negative links with 22 OTUs of 11 genera. These 11 genera all belonged to the anti-*Gardnerella* cooperative alliance expect *Parvimonas* and *Prevotella*, and 6 of them were BVAB. The correlations between these 22 OTUs were all positive. At the species level, it is not only the OTUs of *Aerococcus*, *Atopobium* and *Lactobacillus* that cooperated with *Gardnerella*,

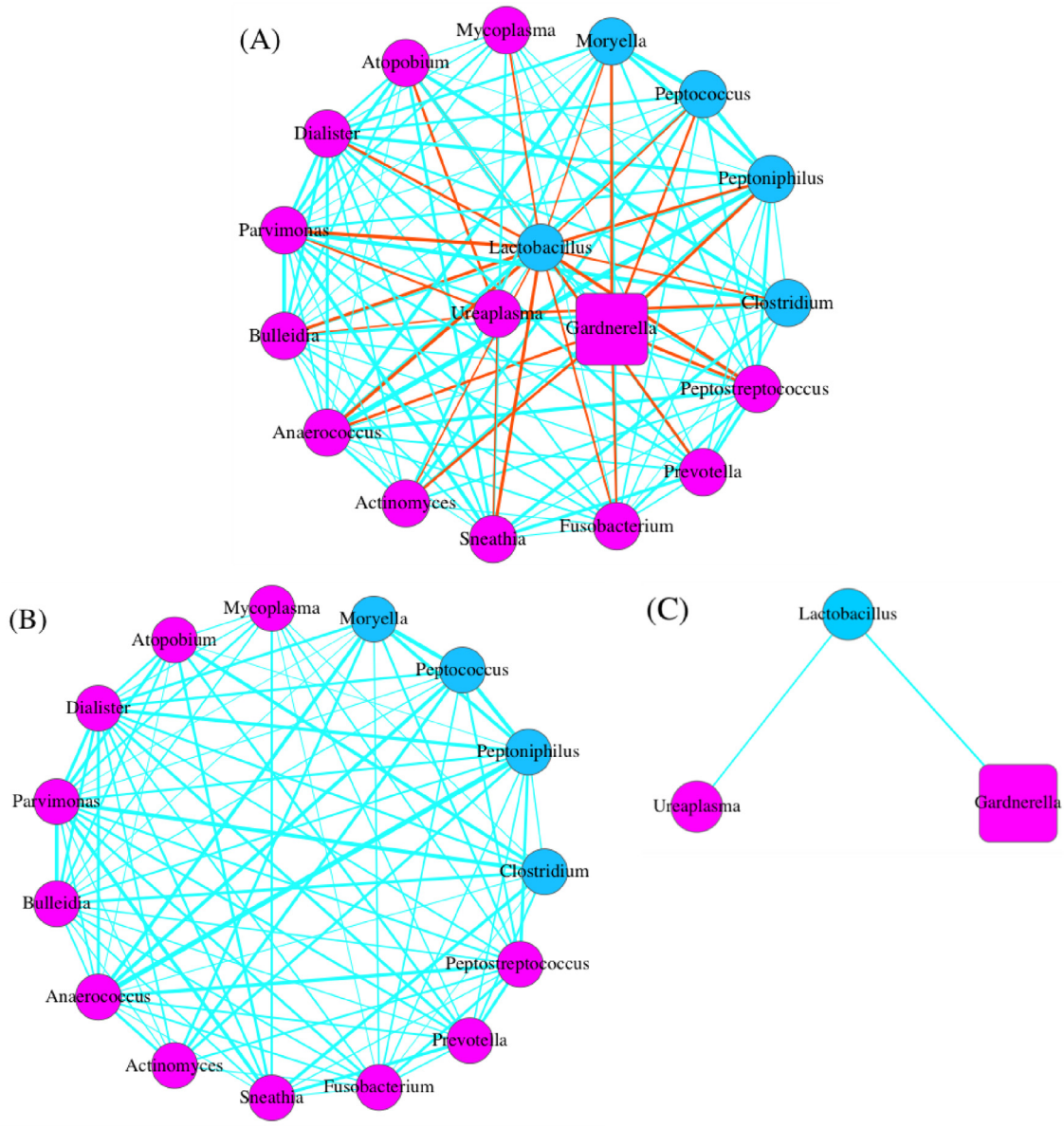

Fig. 5. (A) Sub-network consisting of *Lactobacillus* and directly connected genera in the genus-level DN; (B) Anti-*Lactobacillus* cooperative alliance: network consisting of genera negatively correlated with *Lactobacillus*; (C) *Lactobacillus* cooperative alliance: network consisting of genera positively correlated with *Lactobacillus*. Edges in cyan are positive correlations; edges in orange are negative correlations; the thicker the edge, the stronger the correlated relationship; nodes in magenta are BVAB genera; nodes in sky blue are non-BVAB OTUs; and rectangle represents that the node is both MAO and MDO. (For interpretation of the references to colour in this figure legend, the reader is referred to the web version of this article.)

but also OTUs of other 10 genera, of which 8 were BVAB and 2 were non-BVAB genera. Specifically, in the species-level DN, 20 OTUs were positively correlated with *Gardnerella*, that included *Atopobium vaginae* and *L. iners*.

4. Disscusions and conclusion

Traditionally, the *Lactobacillus*-dominated vaginal microbiome has been associated with health. However, some asymptomatic, otherwise healthy women harbor vaginal microbiomes lacking significant number of *Lactobacillus* species. Although the compositions of these nLDVMs have been intensely studied, the underlying mechanisms of stability remain unclear. Based on the dataset of nLDVMs obtained from 1107 postpartum women in rural Malawi [9], we used the framework of DN analysis to address this mechanistic issue from three aspects, including basic DN structure, core/periphery structure and high-salience skeletons, and the analysis was performed for the genus level microbiome and the microbiome consisting of the dominant species OTUs respectively.

Our study discovered possible mechanisms by which the nLDVM maintain high diversity without absolute predominance of species. We found that the nLDVM was predominantly mutualistic. In both the genus-level and species-level DNs, >90% (93% at the genus level and 91% at the species level) of the competitive (inhibition) relationships were related to the BVABs, of which 60% occurred between BVABs and non-BVABs. It suggested that there is niche overlap between BVABs and non-BVABs and within BVABs, as well as that the resulting competitions could restrict each other to avoid the emergence of a single dominant player in the microbiome. The restriction was mainly embodied in the existence of anti-*Gardnerella* alliance and anti-*Lactobacillus* alliance, and the fact that only a few genera in the genus-level DN cooperated with *Gardnerella* and *Lactobacillus*. Both *Gardnerella* and *Lactobacillus*

have the potential to become the absolute predominance in the vaginal microbiome [39,1,14]. The existence of their corresponding anti-alliances might inhibit the *Gardnerella* and *Lactobacillus* to become the absolute predominance and to maintain the high diversity in the microbiome.

We further determined that the suppressed *Lactobacillus* species were *L. iners* and *L. vaginalis*, and allies of *Lactobacillus* spp. were *Gardnerella* and *Ureaplasma*. The role of *L. iners* in vaginal health remains controversial. *L. iners* is the dominant species of the CST III microbiome that usually occurs during the transitional stage between abnormal and normal, such as post-BV treatment [22,37], but was also frequently found in the microbiome during BV and other vaginal conditions [37,34]. However, our finding of the positive interactions between *L. iners* and BVABs (i.e., *Gardnerella* and *Ureaplasma*) revealed more about the "foe" side of this species. This hypothesis might further be explained by the co-occurrence of *L. iners* and *Gardnerella* spp. that has been found during menses and BV [4]. Studies proposed that *L. iners* AB-1 can strongly adhere to human fibronection and enhance the adhesion of *Gardnerella* spp., which could promote the formation of biofilm and the adhesion of other BV-associated pathogens [4,31,4]. Moreover, *L. iners*, very different from other *Lactobacillus* bacteria, do not produce D-lactic acid and secrete some pathogenic factors, such as inerolysin [32,10,38,30,29]. Inerolysin is similar to vaginolysin encoded by *Gardnerella* spp., which is a cholesterol-dependent and pore-forming cytolysin toxin [38,30,29]. All of these might suggest that *L. iners* acts as an "enemy" in the nLDVMs, and inhibition of *Gardnerella* and *L. iners* might be a self-protective mechanism to maintain stability and health of this microbiome.

However, our finding further indicated that, unlike *L. iners*, *Gardnerella* might be not all bad in the nLDVM, as *Gardnerella* species were positively correlated with both BVABs and non-BVABs. A highly structured polymicrobial biofilm has been found on the vaginal epithelium during BV, which is presumably initiated and predominant by *Gardnerella* spp. [5,3]. We suspected that *Gardnerella* spp. might also play a similar role as an attached scaffold in the construction of the microbiome not dominated by *Lactobacillus* species.

The core-periphery structure can reflect the heterogeneity or asymmetry of OTUs [26,7]. Core represents a densely network entity, which is, intuitively, a set of densely connected, central nodes in the network; periphery refers to a set of sparsely connected, non-central nodes in the network [7]. Both genus and dominant species DN had relatively strong core-periphery structure, indicating the robustness and stability of their structures. This is mainly due to the fact that the rich connection structure of core structure is less prone to degradation and ensures cooperation. We further identified the core/periphery genera and core/periphery dominant species of the nLDVM. In the genus-leve DN, the diversities at orders q = 0–3 of core genera were significant higher than that of periphery genera. However, in the species-level DN, the diversities of core were significant lower than that of periphery. These results suggested that the interactions between dominant species might fluctuate more than those between genera in the nLDVM.

Finally, based on HSS analysis, we identified the high salience skeletons of the DNs and the pathways formed by these skeletons. High salience skeletons can be considered as the "highways" in the complex network, and HSS-pathways might reveal the important exchanges of biomass or essential cooperative/inhibitive interactions in the non-*Lactobacillus* dominated microbiome. Our analyses on genus level found that *Finegoldia* was the hub of the skeletons and *Staphylococcus* was the hub of the HSSs. Analyses on species level were consistent with these results that *Finegoldia* spp. held the most number of skeletons and *S. epidermidis* held the most number of HSSs. *Finegoldia* is normal anaerobic bacteria of the gastrointestinal and genitourinary tract [43]. *S. epidermidis* is the most common species isolated from the human epithelium, which has a benign relationship with its host [36]. What roles that *Finegoldia* spp. and *S. epidermidis* play in the nLDVM will need to be addressed in future studies.

Author Contribution

W.L. performed the data analysis and wrote the paper. Z.M. designed the study and performed interpretations. All authors approved the submission.

Declaration of Competing Interest

The authors declare that they have no known competing financial interests or personal relationships that could have appeared to influence the work reported in this paper.

Acknowledgements

This study received funding from National Science Foundation of China (Grant #31970116); Cloud-Ridge Industry Technology Leader Grant from Yunnan Development and Reform Commission; A grant for genomics/metagenomics big data from Yunnan Science and Technology Bureau.

Appendix A. Supplementary data

Supplementary data to this article can be found online at https://doi.org/10.1016/j.csbj.2020.10.033.

References

[1] Anahtar MN, Byrne EH, Doherty KE, et al. Cervicovaginal bacteria are a major modulator of host inflammatory responses in the female genital tract. Immunity 2015;42:965–76.
[2] Anahtar MN, Gootenberg DB, Mitchell CM, et al. Cervicovaginal microbiota and reproductive health: the virtue of simplicity. Cell Host Microbe 2018;23:159–68.
[3] Alves P, Castro J, Sousa C, et al. Gardnerella vaginalis outcompetes 29 other bacterial species isolated from patients with bacterial vaginosis, using in an in vitro biofilm formation model. J Infect Dis 2014;210(4):593–6.
[4] Castro J, Henriques A, Machado A, et al. Reciprocal interference between Lactoba- cillus spp. and Gardnerella vaginalis on initial adherence to epithelial cells. Int J Med Sci 2013;20:1193–8.
[5] Castro J, Rosca AS, Cools P, et al. Gardnerella vaginalis Enhances Atopobium vaginae Viability in an in vitro Model. Front Cell Infect Microbiol 2020;10:83.
[6] Callahan BJ, DiGiulio DB, Goltsman DSA, et al. Replication and refinement of a vaginal microbial signature of preterm birth in two racially distinct cohorts of US women. Proc Natl Acad Sci U S A 2017;114(37):9966–71.
[7] Csermely P, London A, Wu LY, et al. Structure and dynamics of core/periphery networks. J Complex Networks 2013;1:93–123.
[8] DiGulio DB, Callahan BJ, McMurdie PJ, et al. Temporal and spatial variation of the human microbiota during pregnancy. Proc Natl Acad Sci USA 2015;112:11060–5.
[9] Doyle R, Gondwe A, Fan Y, et al. A Lactobacillus-deficient vaginal microbiota dominates postpartum women in rural Malawi. Appl Environ Microbiol 2018;84(6):e02150–e2217.
[10] Edwards VL, Smith SB, McComb EJ, et al. The cervicovaginal microbiota-host interaction modulates Chlamydia trachomatis infection. MBio 2019;10: e01548–e1619.
[11] Fettweis JM, Brooks JP, Serrano MG, et al. Differences in vaginal microbiome in African American women versus women of European ancestry. Microbiology 2014;160:2272–82.
[12] Fredricks DN, Fiedler TL, Marrazzo JM. Molecular identification of bacteria associated with bacterial vaginosis. N Engl J Med 2005;353:1899–911.
[13] Gajer P, Brotman RM, Bail G, Sakamoto J, et al. Temporal dynamics of the human vaginal microbiota. Sci Transl Med 2012;4(132):132ra52.
[14] Gosmann C, Anahtar MN, Handley SA, et al. Lactobacillus-deficient cervicovaginal bacterial communities are associated with increased HIV acquisition in young South African women. Immunity 2017;46:29–37.
[15] Grady D, Thiemann C, Brockmann D. Robust classification of salient links in complex networks. Nat Commun 2012;3:864.
[16] Hill MO. Diversity and evenness: A unifying notation and its consequences. Ecology 1973;54(2):427–32.

[17] Horner P, Donders G, Cusini M, et al. Should we be testing for urogenital Mycoplasma hominis, Ureaplasma parvum and Ureaplasma urealyticum in men and women? - a position statement from the European STI Guidelines Editorial Board. J Eur Acad Dermatol Venereol 2018;32(11):1845–51.
[18] Huang B, Fettweis JM, Brooks JP, et al. The changing landscape of the vaginal microbiome. Clin Lab Med 2014;34:747–61.
[19] Hyman RW, Fukushima M, Jiang H, et al. Diversity of the vaginal microbiome correlates with preterm birth. Reprod Sci 2014;21:32–40.
[20] Li W, Ma ZS. Diversity scaling of human vaginal microbial communities. Zool Res 2019;40(6):587–94.
[21] Li W, Ma ZS. FBA ecological guild: trio of Firmicutes-bacteroidetes alliance against Actinobacteria in human oral microbiome. Sci Rep 2020;10:287.
[22] Jakobsson T, Forsum U. Lactobacillus iners: a marker of changes in the vaginal flora?. J Clin Microbiol 2007;45:3145.
[23] Kosti I, Lyalina S, Pollard KS, et al. Meta-analysis of vaginal microbiome data provides new insights into preterm birth. Front Microbiol 2020;11:476.
[24] Ma ZS. The P/N (Positive-to-Negative links) ratio in complex networks—a promising *in silico* biomarker for detecting changes occurring in the human microbiome. Microb Ecol 2017. https://doi.org/10.1007/s00248-017-1079-7.
[25] Ma ZS, Ellison AM. A unified concept of dominance applicable at both community and species scales. Ecosphere 2018;9(10):e02477.
[26] Ma ZS, Ellison AM. Dominance network analysis provides a new framework for studying the diversity-stability relationship. Ecol Monogr 2019;89(2):e01358.
[27] Ma ZS, Guan Q, Ye C, et al. Network analysis suggests a potentially 'evil' alliance of opportunistic pathogens inhibited by a cooperative network in human milk bacterial communities. Sci Rep 2015;5:8275.
[28] Ma ZS, Li W. How and why men and women differ in their microbiomes: medical ecology and network analyses of the microgenderome. Adv Sci 2019;6(23):1902054.
[29] Macklaim JM, Fernandes AD, Di Bella JM, et al. Comparative meta-RNA-seq of the vaginal microbiota and differential expression by Lactobacillus iners in health and dysbiosis. Microbiome 2013;1:12.
[30] Macklaim JM, Gloor GB, Anukam KC, et al. At the crossroads of vaginal health and disease, the genome sequence of Lactobacillus iners AB-1. Proc Natl Acad Sci U S A 2011;108:4688–95.
[31] McMillan A, Macklaim JM, Burton JP, et al. Adhesion of Lactobacillus iners AB-1 to human fibronectin: a key mediator for persistence in the vagina?. Reprod Sci 2013;20:791–6.
[32] Mendes-Soares H, Suzuki H, Hickey RJ, et al. Comparative functional genomics of Lactobacillus spp. reveals possible mechanisms for specialization of vaginal lactobacilli to their environment. J Bacteriol 2014;196:1458–70.
[33] Nugent RP, Krohn MA, Hillier SL. Reliability of diagnosing bacterial vaginosis is improved by a standardized method of gram stain interpretation. J Clin Microbiol 1991;29:297–301.
[34] Nunn KL, Wang YY, Harit D, et al. Enhanced trapping of HIV-1 by human cervicovaginal mucus is associated with Lactobacillus crispatus-dominant microbiota. MBio 2015;6:e01084–e1115.
[35] Onderdonk AB, Delaney ML, Fichorova RN. The human microbiome during bacterial vaginosis. Clin Microbiol Rev 2016;29(2):223–38.
[36] Otto M. Staphylococcus epidermidis–the 'accidental' pathogen. Nat Rev Microbiol 2009;7(8):555–67.
[37] Petrova MI, Reid G, Vaneechoutte M, Lebeer S. Lactobacillus iners: friend or foe?. Trends Microbiol 2017;25(3):182–91.
[38] Rampersaud R, Planet PJ, Randis TM, et al. Inerolysin, a cholesterol-dependent cytolysin produced by Lactobacillus iners. J Bacteriol 2011;193(5):1034–41.
[39] Ravel J, Gajer P, Abdo Z, Schneider GM, et al. Vaginal microbiome of reproductive-age women. Proc Natl Acad Sci 2011;108:4680–7.
[40] Ravel J, Brotman RM, Gajer P, et al. Daily temporal dynamics of vaginal microbiota before, during and after episodes of bacterial vaginosis. Microbiome 2013;1:29.
[41] Romero R, Hassan SS, Gajer P, et al. The composition and stability of the vaginal microbiota of normal pregnant women is different from that of non-pregnant women. Microbiome 2014;2:4.
[42] Rosca AS, Castro J, Sousa LGV, et al. Gardnerella and vaginal health: the truth is out there. FEMS Microbiol Rev 2020;44:73–105.
[43] Rosenthala ME, Rojtmanb AD, Franka E. Finegoldia magna (formerly Peptostreptococcus magnus): An overlooked etiology for toxic shock syndrome?. Med Hypotheses 2012;79(2):138–40.
[44] Shannon P, Markiel A, Ozier O, et al. Cytoscape: a software environment for integrated models of biomolecular interaction networks. Genome Res 2003;13:2498–504.
[45] Stout MJ, Zhou Y, Wylie KM, et al. (2017) Early pregnancy vaginal microbiome trends and preterm birth. American Journal of Obstetrics and Gynecology, 217 (3): 356.e1–e18.
[46] Taylor-Robinson D. Mollicutes in vaginal microbiology: Mycoplasma hominis, Ureaplasma urealyticum, Ureaplasma parvum and Mycoplasma genitalium. Res Microbiol 2017;168:875–81.